The Cornet seismological network: 10 years of operation, recorded seismicity and significant applications*

Panayotis Papadimitriou, George Kaviris, Andreas Karakonstantis & Kostas Makropoulos
Department of Geophysics, Faculty of Geology & Geoenvironment, University of Athens, Panepistimiopolis, 157 84, Zographou, Athens, Greece
ppapadim@geol.uoa.gr, gkaviris@geol.uoa.gr, akarakon@geol.uoa.gr, kmacrop@geol.uoa.gr

ABSTRACT: The Gulf of Corinth is a region characterized by intense deformation and very high seismic activity. The latter is expressed by the occurrence of both microearthquakes and large events which have caused severe damage since the antiquity. The installation of the Cornet seismological network in 1995 by the Seismological Laboratory of the University of Athens contributed to the detailed recording of the seismicity, as well as to the achievement of various research interests. Furthermore, the Seismological Laboratory, in cooperation with international institutes, installed during the last three decades around the Gulf of Corinth temporary local networks either to monitor microseismic activity or to record aftershock sequences. The determination of the source parameters and the hypocenter relocation for the events that occurred in the broader area of the Gulf of Corinth contributed to the highlighting of the main active faults, as well as of the stress field. The NNE-SSW extension was pointed out through the focal mechanisms that were determined for moderate earthquakes. A significant number of relocated hypocenters was clustered, while the seismogenic layer was determined between 10 and 15 km depth. Anisotropy study, performed in the eastern part of the Gulf using recordings of the Cornet network, revealed an anisotropic upper crust related to the stress field of the region. Recently, the Cornet Network was gradually replaced by the Athenet seismological Network that is part of the Hellenic Unified Seismological Network (HUSN), whose data are used to calculate and publish earthquake source parameters in real-time.
Key words: *Gulf of Corinth, Greece, Seismological Networks, Seismicity, Velocity Model, Source Parameters, Anisotropy, Relocation*.

ΠΕΡΙΛΗΨΗ: Ο Κορινθιακός Κόλπος χαρακτηρίζεται από έντονη παραμόρφωση και ιδιαίτερα υψηλή σεισμική δραστηριότητα που εκδηλώνεται με τη γένεση τόσο μικροσεισμών, όσο και ισχυρών σεισμών οι οποίοι έχουν προκαλέσει σοβαρές καταστροφές από την αρχαιότητα μέχρι σήμερα. Η απουσία μόνιμων σεισμολογικών σταθμών στον Κορινθιακό Κόλπο οδήγησε το Εργαστήριο Σεισμολογίας του Πανεπιστημίου Αθηνών στην εγκατάσταση του σεισμολογικού δικτύου Cornet το 1995, το οποίο συνέβαλε τόσο στην καταγραφή της μικροσεισμικής δραστηριότητας της περιοχής, όσο και στην επίτευξη περαιτέρω ερευνητικών στόχων. Επιπλέον, το Εργαστήριο Σεισμολογίας του Πανεπιστημίου Αθηνών εγκατέστησε σε συνεργασία με άλλα ερευνητικά ινστιτούτα, κατά τη διάρκεια των τελευταίων τριών δεκαετιών, προσωρινά τοπικά δίκτυα γύρω από τον Κορινθιακό Κόλπο, είτε για την παρακολούθηση της μικροσεισμικής δραστηριότητας, είτε για την καταγραφή μετασεισμικών ακολουθιών. Ο προσδιορισμός των εστιακών παραμέτρων και ο επαναπροσδιορισμός υποκέντρων, σε συνδυασμό με μηχανισμούς γένεσης για τους σεισμούς που συνέβησαν στην ευρύτερη περιοχή του Κορινθιακού Κόλπου, συνέβαλαν στην ανάδειξη των ενεργών ρηγμάτων, καθώς και του πεδίου τάσεων. Η ΒΒΑ-ΝΝΔ διεύθυνση επέκτασης εντοπίστηκε μέσω της συγκέντρωσης των επικέντρων των επιφανειακών σεισμών και των μηχανισμών γένεσης που καθορίστηκαν για σεισμούς ενδιαμέσου μεγέθους. Το σεισμογόνο στρώμα εντοπίστηκε σε βάθη μεταξύ 10 και 15 χλμ. Η μελέτη ανισοτροπίας, που διεξήχθη στο ανατολικό τμήμα του Κόλπου χρησιμοποιώντας καταγραφές του δικτύου Cornet, ανέδειξε έναν ανισοτροπικό ανώτερο φλοιό που σχετίζεται άμεσα με το πεδίο τάσεων της περιοχής. Πρόσφατα, το δίκτυο Cornet αντικαταστάθηκε βαθμιαία από το δίκτυο Athenet που αποτελεί τμήμα του Ελληνικού Ενιαίου Σεισμολογικού Δικτύου (HUSN), με τα δεδομένα του οποίου υπολογίζονται και παρουσιάζονται οι εστιακές παράμετροι σε πραγματικό χρόνο.
Λέξεις-κλειδιά: *Κορινθιακός Κόλπος, Ελλάδα, Σεισμολογικά Δίκτυα, Σεισμικότητα, Μοντέλο Ταχύτητας, Σεισμικές Παράμετροι, Ανισοτροπία, Επαναπροσδιορισμός Υποκέντρων*.

INTRODUCTION

The Gulf of Corinth is considered to be one of the most active tectonic rifts around the world. Seismological and tectonic studies indicate that the morphology of the Gulf of Corinth is mainly due to repeated earthquakes that have generally occurred on 40° to 60° north-dipping normal faults. The Gulf is characterized by the long term subsidence of the northern coast and upward displacement of the main footwalls. The mean extension rates of the Gulf are significantly high and reach 14 mm/yr in the west, 13 mm/yr in the center and 10 mm/yr in the east, in an almost N-S direction (Billiris *et al*., 1991; Briole *et al*., 2000). This rapid extension is associated with a very young phase of faulting (~ 1 Ma) cutting an older extensional basin (Armijo *et al*., 1996).

The eastward progressive width and depth increase, which coincides with an increase of the sediment infill, suggests that the amount of extension across the central-eastern part of the Gulf is greater than at the western boundary (Brooks & Ferentinos, 1984; Armijo *et al*., 1996). The faulting geometry at the eastern boundary of the Gulf of Corinth seems to have changed since the initiation of the rifting process. Fault activity appears to have migrated northwards, as in the western and central parts of the Rift, but the orientation of the faults has also changed. The newer fault steps are oblique to the older faults and basins, a geometry that has given rise to recently deformed palaeogeographic markers (Armijo *et al*., 1996). The major and most active

* Σεισμολογικό δίκτυο Cornet: 10 χρόνια λειτουργίας, σεισμικότητα και σημαντικές εφαρμογές

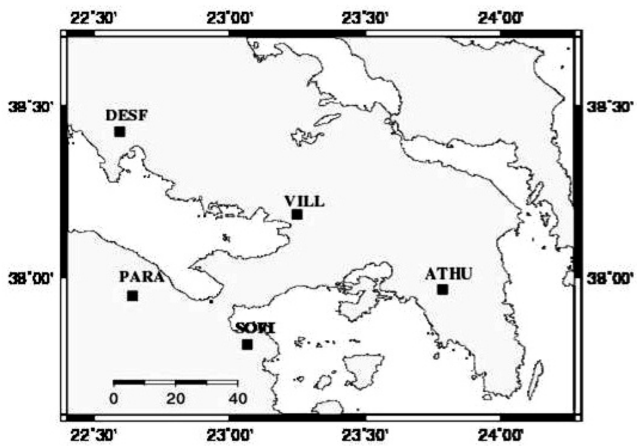

Fig. 1. The permanent digital Cornet Telemetric Network.

TABLE 1
Stations of the Cornet Network.

Station Name	Location	Longitude (ºE)	Latitude (ºN)	Altitude (m)
Athu	Athens	23.785	37.962	307
Desf	Desfina	22.594	38.425	983
Para	Paradisi	22.640	37.947	782
Sofi	Sofiko	23.064	37.805	719
Vill	Villia	23.247	38.184	1384

faults at the eastern edge of the present Corinth Rift are situated north of the basins of Corinth Isthmus and Megara, in continuity with the main en echelon normal fault segments that bound the high relief along the southern coast of the Gulf and have a N70-90°E strike.

The Gulf of Corinth has experienced several large earthquakes that destroyed some of the ancient cities, such as Heliki, Corinth, Delphi and Patras in historical times (Papazachos & Papazachou, 1989). Since the beginning of instrumental seismology, six earthquakes of M>6 were located around the Gulf of Corinth, most of them at its eastern part end, close to the city of Corinth. Most focal mechanisms reveal a consistent pattern of E-W trending normal faulting, with one plane dipping shallowly towards the north. The occurrence of significant earthquakes in the 80's (Alkyonides-Kaparelli) and 90's (Galaxidi and Aigion) revealed the necessity to install a permanent network in the area of the eastern Gulf of Corinth in order to monitor the seismic activity and determine source parameters as accurately as possible. In 1995, the Seismological Laboratory of the University of Athens installed the Cornet seismological permanent network around the eastern Gulf of Corinth (Papadimitriou *et al*., 1996). This network consisted of digital telemetric Lennartz stations with L4 and Le-3D (1 Hz) seismometers, recording with a sampling rate of 125 samples/sec (Papadimitriou *et al*., 1999).

Main results around the broader Gulf of Corinth are presented in order to reveal the importance of seismic monitoring in such tectonically active regions. Anisotropy study was performed in the area of the Eastern Gulf of Corinth, taking advantage of the Cornet seismological network recordings. The presence of this network was crucial for the increase of well-located events into this area and significantly helped the relocation process. A local velocity model was developed through minimization of residuals. Furthermore, the duration magnitude M_D and the moment magnitude M_w (using spectral analysis) were calculated, while relationships between them, the local M_L and the body-wave m_b magnitudes were determined throughout the operation of the Cornet seismological network and will be referred in the following paragraphs of this study.

CORNET NETWORK

The Cornet telemetric seismological network was installed, since 1995, by the Seismological Laboratory of the Geophysics – Geothermics Department of the University of Athens (Papadimitriou *et al*., 1996; Kaviris, 2003; Kaviris *et al*., 2007). This network, which is the first digital permanent network in Greece, operated in a region of continuous seismic activity characterized by normal faulting with an approximately E-W direction. The area was chosen due to its high seismicity, while no permanent seismological stations existed in the region of interest. Furthermore, the east Gulf of Corinth has been affected by several destructive earthquakes, the most recent of which is the Alkyonides earthquake sequence of 1981 (Jackson *et al*., 1982). The relatively small distance between the Alkyonides Gulf and Athens makes this area a source of seismic risk for the capital of Greece.

The network initially consisted of 5 stations (Fig. 1), but due to hardware limitations only 4 operated. At the beginning 3D/1Hz seismometers were installed at each station. Following, they were replaced with LE-3D/5sec Lennartz seismometers. The station coordinates of the Cornet network are presented in Table 1. The network was also equipped with a Lennartz 5800 PCM central system. The recorded signals were transmitted directly or through repeaters to the central station, located in the premises of the Faculty of Geology and Geoenvironment of the University of Athens, via antennas at predefined frequencies. The main goal of installation of the network was the recording of all local events and the determination of their source parameters with the best possible accuracy.

VELOCITY MODEL

The calculation of a reliable velocity model needs, as a starting point, an initial model that will be modified. In the case of the Cornet network the one obtained by Rigo *et al*. (1996) was used for the preliminary location of the events. Following, the Chatelain method, that takes into account all events, was used for the Vp/Vs ratio determination. The events located mainly within the Eastern Gulf of Corinth were used for that purpose. For every pair (i, j) of stations the differences of the P and of the S arrival times are calculated. The Vp/Vs ratio is given by the equation:

$$Vp/Vs = (ts_j - ts_i) / (tp_j - tp_i) \qquad (1)$$

The obtained points are plotted in Fig. 2 and using the Least Squares Method the Vp/Vs ratio was found equal to 1.79. This value was the same both when all the events in the above-mentioned area were used and when selection criteria, relevant to location errors, were applied. This value is in agreement with the Vp/Vs ratio obtained in neighboring areas, varying between 1.77 and 1.83 (Melis *et al.*, 1989; Rigo *et al.*, 1996). In the present study the velocity model was calculated using the rms minimization method for each seismic layer (Crosson, 1976). The events used for that purpose fulfilled the following criteria: a.) Area: within the network, b.) Number of Phases ≥ 6 and c.) rms<0.3 sec, erh<5 km, erz<5 km. The obtained dataset formed a representative sample both in vertical and horizontal distribution. The velocity model that consisted of six (6) seismic layers (Table 2) was calculated and led to the best possible determination of source parameters. The obtained model was verified using a larger dataset with similar results. The velocity model was also compared, giving more satisfactory results (smaller location errors), with the one determined by Rigo *et al.* (1996) for the West Gulf of Corinth.

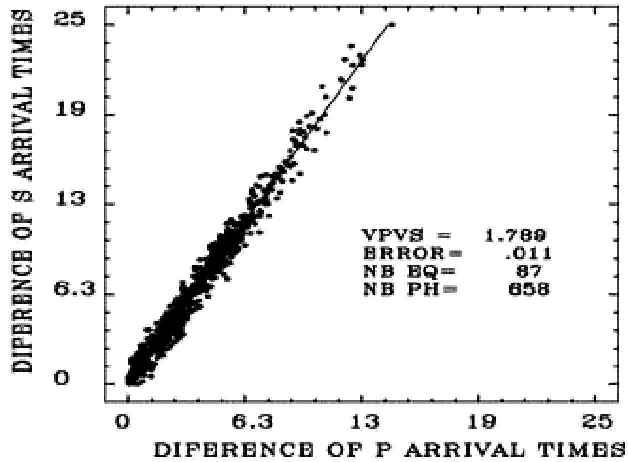

Fig. 2. Vp/Vs Ratio Estimation.

TABLE 2
Velocity Model.

Velocity Vp (km/sec)	Depth (km)
4,5	0,0
5,5	1,3
5,7	4,2
6,1	7,0
6,3	11,5
6,5	16,5
7,0	30,0

MICROSEISMIC ACTIVITY

The Eastern part of the Gulf of Corinth has a key role in the active tectonics of Central Greece. The high slip rates measured and the significant earthquakes that occurred in the previous decades in the region are not in accordance with the relatively low seismicity in the available earthquake catalogues during the period of operation of the Cornet network. The installation of this network in the areas that surround the Eastern Gulf of Corinth contributed to the monitoring of earthquakes, even with M<2. For the period 1995-2004, 6.371 events were located by the Cornet network, more than 2.500 of which in the Eastern Gulf of Corinth. The major part of the seismicity is located within the Gulf (Fig. 3a). A cluster is situated in the Galaxidi area, close to the epicenter of the mainshock of the 18th November 1992 (M=6.2). The significant clustered microseismic activity north of Xylokastron can be related to the western edge of the Alkyonides fault activated on 24 February 1981, an area where no large earthquake has occurred during the last decades. High rates of seismicity are also observed in the Perachora peninsula, Porto

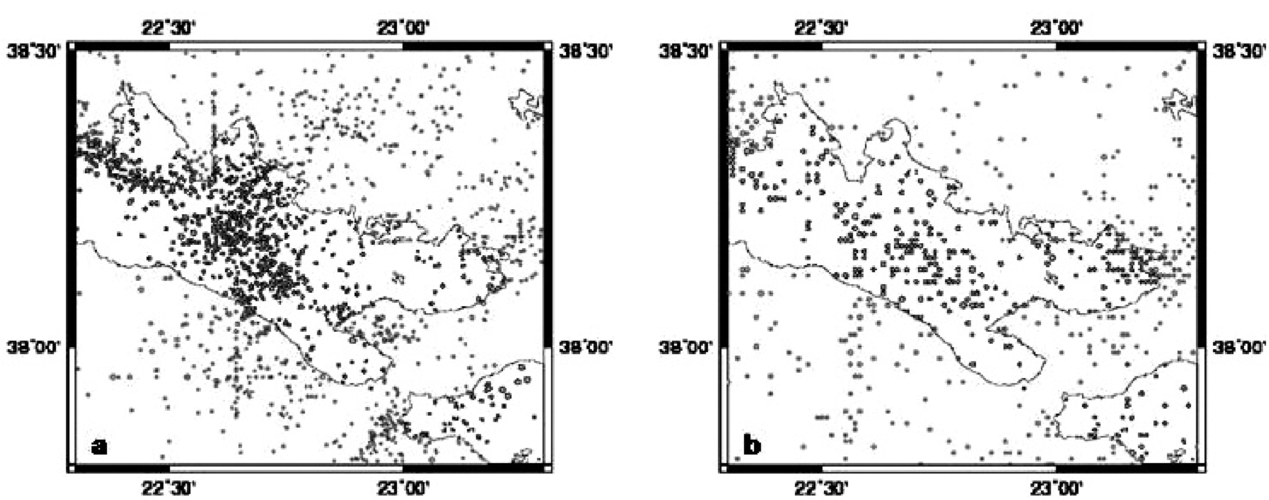

Fig. 3. Seismicity located by a) Cornet Network and b) G.I-N.O.A.

Germeno and Sofiko regions. The seismicity provided by the GI-NOA catalogue for the same period is presented in Fig. 3b, where the microseismic activity is only partially represented.

The phases of the Cornet Network of the National and Kapodistrian University of Athens, the Institute of Geodynamics of the National Observatory of Athens (GI-NOA) and the Department of Geophysics of the Aristotle University of Thessaloniki (AUTH) were merged in order to obtain a complete (joint) catalogue with more accurate hypocenter locations. This procedure contributed to the concentration of the hypocenters in more accurate depths and to the reduction of their spatiotemporal errors. In the study area 1.314 events with $M \geq 2.0$ were relocated with HYPODD, giving a first result that could be rated as satisfactory. The mean temporal errors (rms) were reduced from 0.53 sec to 0.28 sec while the spatial errors (erx, ery, erz) were differentiated from 2.4, 1.8 and 6.9 km to 2.8, 3.6 and 4.3 km, respectively (Fig. 4a, b). Even though a small increase in horizontal errors is observed, a more satisfactory concentration of the hypocenters is obtained. These data were also processed by HYPOINVERSE, where 894 events were relocated in an even better location (Fig. 4c, d). The mean temporal residual (rms) that was determined by HYPOINVERSE was 0.18 sec, while the respective one obtained by the relocation process was 0.08 sec. During the procedure of location with HYPOINVERSE, the spatial errors reached 3.5, 4.8 and 13.1 km (erx, ery, erz). The respective spatial errors obtained by the relocation procedure using the double-difference algorithm (HYPODD) were smaller than 1.5 km. The epicentres are concentrated along the active normal faults of the region. Earthquake locations are clustered in areas close to Xylokastron, Galaxidi and Perachora peninsula. Furthermore, the artefact epicentral solutions by HYPO71 (Fig. 4a) aligned in N-S and E-W directions are not present after the relocation procedure (Fig. 4b).

DETERMINATION OF DURATION MAGNITUDE

The determination of reliable magnitudes was one of the main objectives of the installation of the Cornet network. The calculation of the local (M_L), the surface (M_s) and the body wave (m_b) magnitude is based on the measurement of the amplitude A and of the period T. The accurate amplitude determination using a certain frequency range of the waveform presents difficulties due to waveform complexities, leading in certain cases to incorrect magnitude determination. On the other hand, the advantages of the duration magnitude are that only one parameter, the total signal duration, is used and that it is rapidly calculated. For all the above mentioned reasons, several studies have been performed in Greece for its deter-

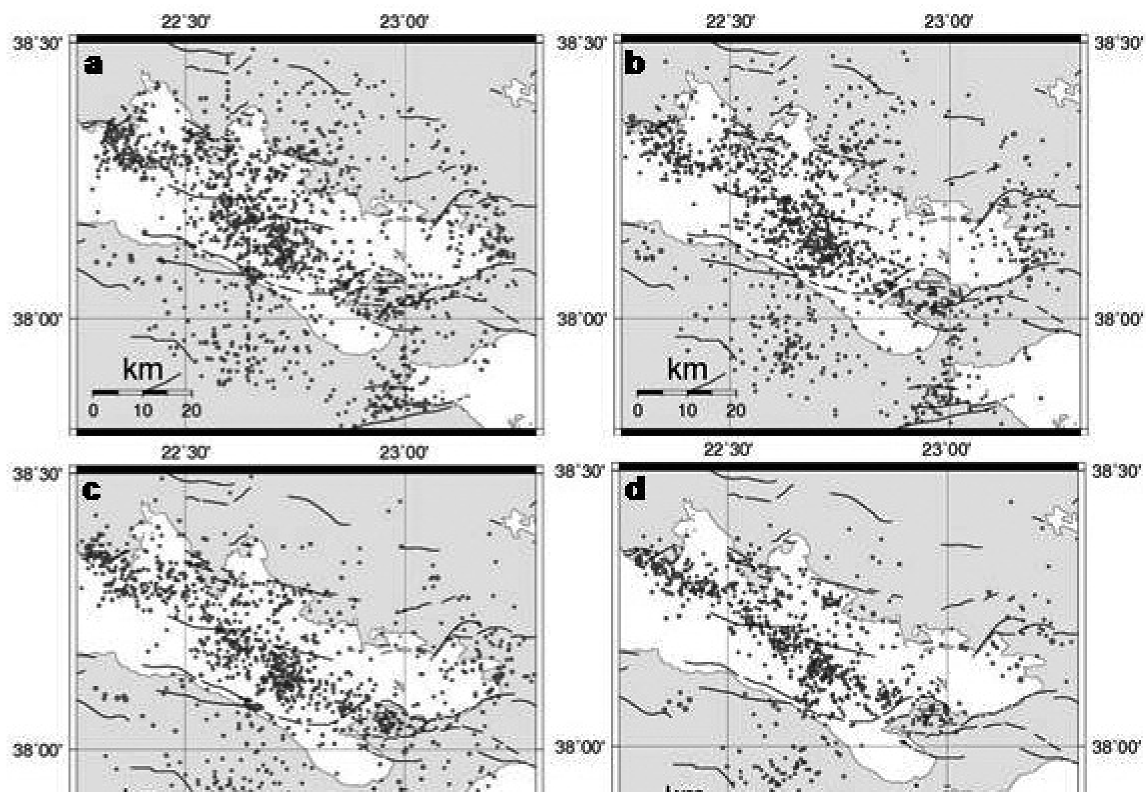

Fig. 4. Epicenters a) Located with HYPO71, b) Relocated with HYPODD using a HYPO71 processed catalogue, c) Located with HYPOINVERSE, d) Relocated with HYPODD using a HYPOINVERSE processed catalogue.

mination (KIRATZI, 1984; PAPANASTASIOU, 1989; TSELENTIS, 1997). However, it should be noted that discrepancies can be observed concerning the determination of the total signal duration. Nevertheless, in the present study the duration measurements were cross-checked, either with similar observations or by comparing them with the respective moment magnitudes.

The duration magnitude M_D is one of the most commonly used magnitude scales for local networks and is calculated using the formula:

$$M_D = \alpha + \beta \cdot \log D + \gamma \cdot \Delta \quad (2)$$

where D is the total signal duration in sec (until the signal to noise ratio is equal to 1), Δ is the epicentral distance in km and α, β, γ constants. The main step for a reliable duration magnitude was the determination of the constants α, β and γ. A methodology was developed for their determination using linear multiple regression. Whence, the obtained formula is:

$$M_D = -1.1 + 2.35 \cdot \log D + 0.0012 \cdot \Delta \quad (3)$$

It should be noted that the selected dataset consisted of earthquakes for which both the local magnitude (M_L), calculated by GI-NOA, and the body wave magnitude m_b, calculated by the ISC, were available. The epicentral distances of these events varied between 10 and 200 km.

DETERMINATION OF MOMENT MAGNITUDE

The next goal was the determination of the moment magnitude M_W which is based on the calculation of a physical quantity, the seismic moment. This is considered to be the most reliable magnitude scale, since it is not saturated and does not depend on the frequency window. The calculation of the low-frequency spectral level Ω_0, as well as of the corner frequency, were performed using spectral analysis. Following, the seismic moment M_0 is determined by the equation:

$$M_0 = \frac{4\pi\rho\beta^3 R\Omega_0}{R_{rp}} \quad (4)$$

where ρ is the density, β the S-wave velocity, R the hypocentral distance and Rrp is the S-wave radiation pattern coefficient, which in the present study is considered equal to 0.85. Following, the moment magnitude M_W is calculated as (HANKS & KANAMORI, 1979):

$$M_W = \frac{2}{3}\log M_0 - 10.73 \quad (5)$$

An earthquake catalogue was created, where the moment magnitude M_W was directly calculated by processing digital data. As an example, the response spectra of the Desfina (component E-W) and the Sofiko (component N-S) stations of an earthquake that occurred on 19 February 1997 are presented in Fig. 5. After the determination of the spectral amplitude Ω_0, the value of the seismic moment was found equal to $M_0=1\cdot10^{23}$ dyn•cm, resulting a moment magnitude M_W=4.6. Furthermore, the corner frequency is f_0=2 Hz which corresponds to a duration of the source time function equal to 0.5 sec.

After the independent calculation of both the moment magnitude M_W and the duration magnitude M_D, using data recorded by the Cornet network, the following relationship between them was obtained, using linear regression:

$$M_W = 0.99\, M_D + 0.61 \qquad \text{for } 3.0 \leq M_D \leq 4.5 \quad (6)$$

This equation is similar with the one obtained by PAPAZACHOS *et al.* (1997) for Greece:

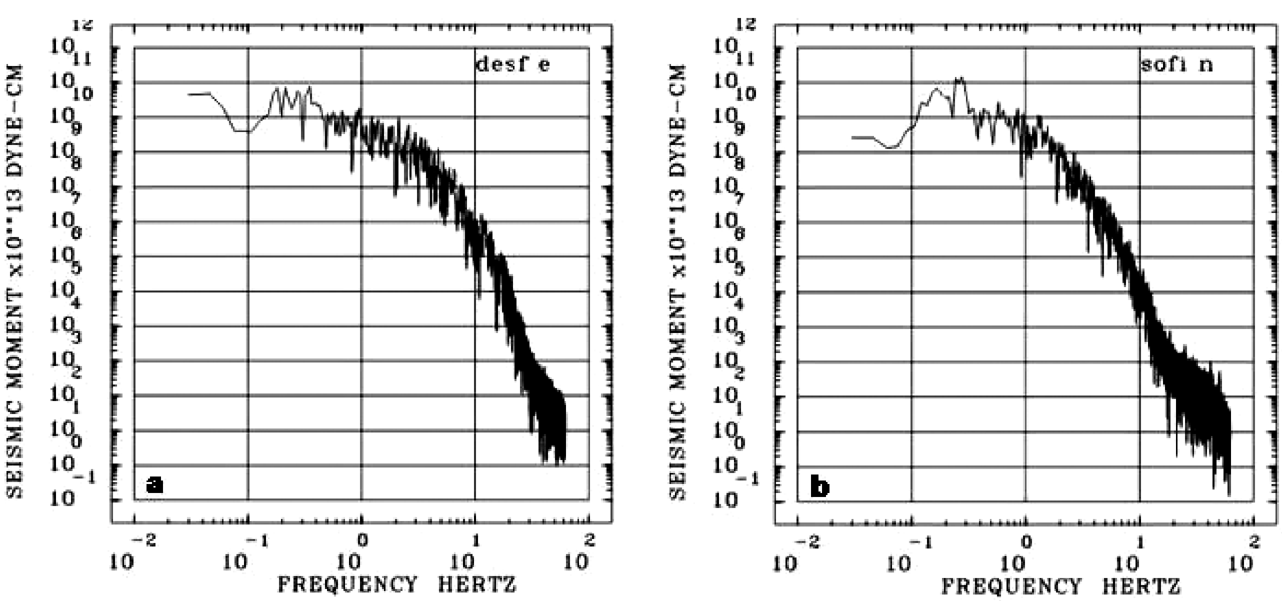

Fig. 5. Spectral analysis of the 19 February 1997 event for the calculation of the seismic moment using recordings of a) Desfina and b) Sofiko stations.

$M_W = 0.97\ M_L + 0.58, \quad \text{where } M_L = M_D \qquad (7)$

The relation obtained in the framework of the present study can be replaced by the:

$$M_W = M_D + 0.6 \qquad (8)$$

which is more practical and gives the same results. Using linear regression, relations between the moment magnitude M_w and the local magnitude M_L (GI-NOA), the body wave magnitude m_b (ISC) and the seismic energy E were obtained:

$$M_W = 0.63\ M_L + 2.04 \qquad \text{for } 2.8 \le M_L \le 4.9 \qquad (9)$$

$$M_W = 0.77\ m_b + 1.37 \qquad \text{for } 3.2 \le m_b \le 4.8 \qquad (10)$$

$$\log E = 1.61\ M_W + 7.97 \qquad \text{for } 3.3 \le M_W \le 5.3 \qquad (11)$$

ANISOTROPY STUDY

Understanding the geometry and evolution of fracture systems in the anisotropic upper crust is a fundamental problem in geomechanics. Several studies of local earthquakes performed in various sedimentary and crystalline geological regimes, below some critical depth, revealed the existence of shear-wave splitting (e.g. Kaneshima, 1990; Papadimitriou *et al*., 1999; Hao *et al*., 2008). In all the above mentioned studies, the shear-wave splitting phenomenon has been related to the existence of anisotropic medium (Crampin, 2003). When an approximately vertical shear wave propagates through effectively anisotropic media, it splits into two components with different velocities: the S_{fast} and the S_{slow}. These two shear waves have different arrival times and nearly orthogonal polarizations. The observed time delay between the two split shear waves defines the magnitude of anisotropy and is related to the crack density and aspect ratio, as well as to the length of the ray path in the anisotropic medium. Various models have been proposed to explain the observed seismic anisotropy, one of which is the extensive dilatancy anisotropy (EDA) based on aligned cracks and microcracks (Crampin, 1978) which preferentially align with the current stress field, parallel to the maximum horizontal compressive stress. Such results have been obtained for the western Gulf of Corinth, (Bouin *et al.*, 1996; Kaviris *et al.*, 2008) and for other regions worldwide, as Iceland (Crampin *et al.*, 1999) and China (Gao *et al.*, 1998).

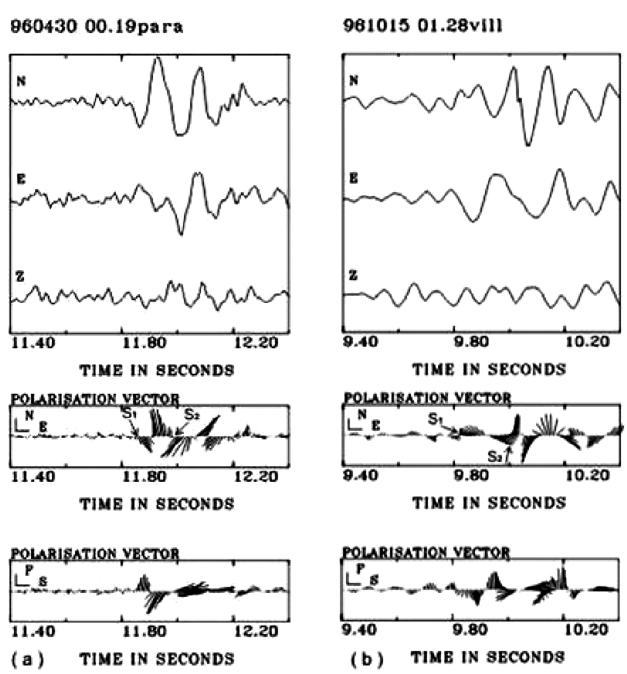

Fig. 6. a) Three component seismograms of an earthquake recorded at Paradeisi station. The original traces are presented at the top of the figure. In the middle the polarization vector is presented in the N-E plane where the polarization directions of the fast (S_1) and the slow (S_2) shear waves are indicated. At the bottom, the polarization vector of the rotated waveforms is presented in the fast-slow plane, b) Same as Figure 6a for an earthquake recorded at Villia station.

As it was shown in Fig. 3a many events were located very close to one of the Cornet stations. Thus, a data set suitable for anisotropy study was chosen. All these events are located close (t_{s-p}<2,5sec) to one of the Cornet stations and were selected to have incident angles smaller than the critical angle in order to avoid the S to P converted phases (Booth & Crampin, 1985). To verify the azimuth and the angle of incidence of the selected events, they were also estimated using a methodology developed for that purpose, based on the Kanasewich (1981) method for the first P-wave window, as well as the polarization of the first P-wave motion recorded in the three components. The selected events have clear and impulsive S wave arrival phases on the horizontal components. In addition, the amplitude of the S wave phase on the vertical component is smaller than on the horizontal ones. The methods used for the determination of the splitting parameters are the polarigram and, in cases where the polarization direction of the fast split shear wave was close to N90°, the hodogram. Initially, the direction of polarization of the medium was calculated. Following, the waveforms were rotated to the fast and slow direction, respectively, and the time delay between the two split shear waves was measured to estimate the magnitude of anisotropy.

In Fig. 6, two events recorded by different Cornet stations are presented. For the first event, recorded by the Paradeisi station (Fig. 6a), the polarization direction, which is the angle between the north and the fast axis direction, is measured on the polarigram of the N-E plane and is equal to N140°. Then the seismograms are rotated in the fast and slow direction and the obtained polarigram is also presented in Fig. 6a. In this figure the obtained polarization vector is oriented almost parallel to the fast component. The measured time delay between the two split shear waves is equal to 0.080sec and represents the magnitude of anisotropy. The same procedure was followed for the Villia station and an example is shown in Fig. 6b. The measured S_{fast} polarization direction is N125°. The waveforms are rotated to the S_{fast} polarization direction to estimate the time delay, which is equal to dt = 0.176 sec.

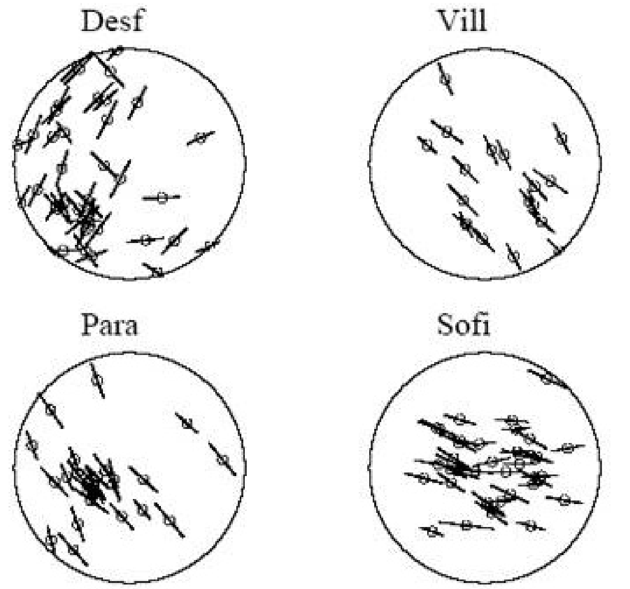

Fig. 7. Polar equal-area projections on the upper hemisphere of the fast shear wave polarizations measured at each Cornet station.

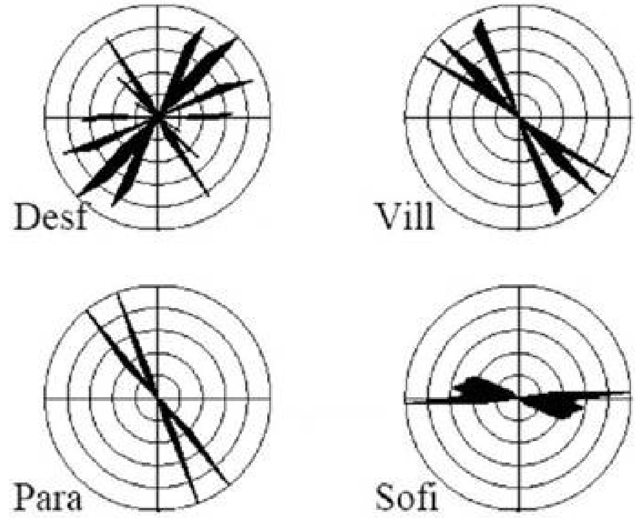

Fig. 8. Rose diagrams of the fast shear wave polarization directions at the Cornet stations.

The S_{fast} polarization directions for each Cornet station are presented on equal-area projections of the upper hemisphere in Fig. 7. The outer circle defines the S-wave window and represents an angle of incidence of 45°. The length of the bars is proportional to the time delay between the fast and slow shear waves. The values of the time delays for the 75 events analyzed at Sofiko station vary between 0.024 sec and 0.160 sec, while the polarization directions of the fast shear wave between N78° and N126°. The coherence of the fast shear wave polarizations at Sofiko station, irrespective of the azimuth of each event, is consistent with shear-wave splitting due to the seismic wave propagation through an anisotropic medium. The same observation is evident for the Paradeisi and Villia stations. The values of the time delays at Paradeisi station, where 47 events were analyzed, vary between 0.024 sec and 0.128 sec, while at Villia station (57 analyzed events) between 0.040 sec and 0.184 sec. The polarization directions of the fast shear wave at Paradeisi station vary between N125° and N165°, while at Villia station between N125° and N163°. For Desfina station the 101 events that were analyzed present more complicated results, as the shear wave polarizations present two different and quasi-perpendicular main directions. The values of the time delays at Desfina station vary between 0.016 sec and 0.096 sec, while the polarization directions of the fast shear wave vary between N16° and N160°. Comparing the calculated time delays, we observe that they have higher values in the stations situated in the eastern part of the Gulf (Sofiko and Villia).

The S_{fast} polarization directions at each Cornet station are presented in Fig. 8 using equal-area rose diagrams. The mean direction at Sofiko station is N106º ± 13º. At Paradeisi station we observe two directions of anisotropy with a mean value equal to N142º ± 13°, while at Villia station there are three directions with a mean value equal to N142° ± 10°. Finally, at Desfina station various directions of anisotropy are observed (Papadimitriou *et al*., 1999). However, two main directions are distinguished, approximately N55° and N143°. The mean values of the anisotropy direction of each station are presented in Fig. 9. The mean polarization directions at Paradeisi, Villia and Desfina (main direction) stations are similar and equal to N142°, while the one measured at Sofiko station (N106°) is more East–West, possibly influenced by

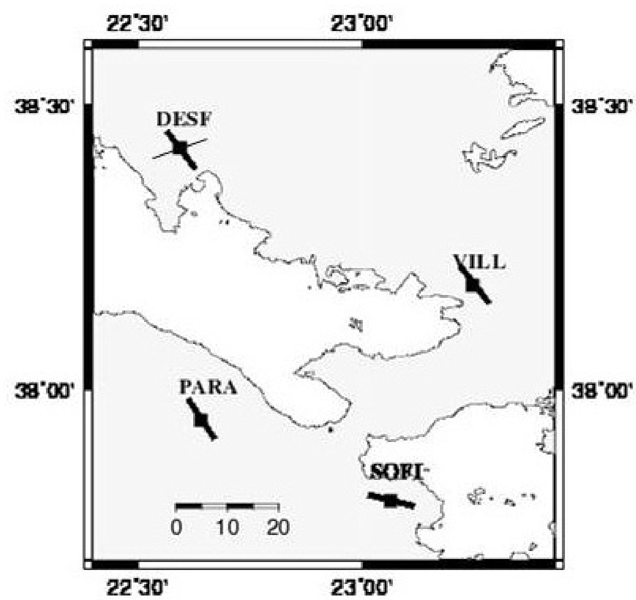

Fig. 9. Mean S_{fast} polarization directions at the Cornet stations (thick bars). The secondary mean S_{fast} polarization direction calculated at Desfina station is also presented (thin bar).

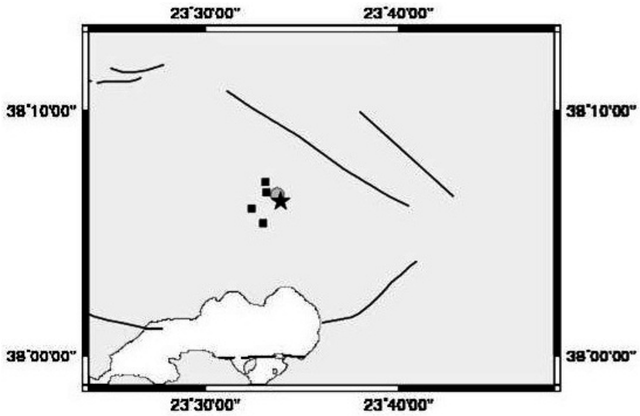

Fig. 10. The relocated epicenters of the mainshock (star) and of the four foreshocks (squares) are shown. The circle represents the epicenter of the aftershock used as master event for the relocation procedure.

TABLE 3
Locations and magnitudes of the Athens earthquake reported by different institutes.

Date	Time (GMT)	Lat. (°) N	Lon. (°) E	Depth (km)	M_S	M_w	Institute
1999-09-07	11:56:50.8	38.105	23.565	9		6.0	NKUA
1999-09-07	11:56:50.5	38.150	23.620	30	5.9		NOA
1999-09-07	11:56:49.3	38.132	23.545	10	5.6	5.9	USGS
1999-09-07	11:56:49.3	38.119	23.605	10	5.8	6.0	PDE
1999-09-07	11:56:49.4	38.120	23.600	10		6.0	HRV

the Saronicos Gulf stress field as well. These observations are consistent with the dynamic field of the Gulf, characterized by a general NNE-SSW direction of extension and, therefore, in agreement with the extensive dilatancy anisotropy (EDA) model, according to which (Crampin, 1978) microcracks, cracks, fractals and pore spaces will preferentially align with the current stress field, parallel to the maximum horizontal compressive stress.

THE ATHENS 1999 EARTHQUAKE

On September 7, 1999 a destructive earthquake occurred in Thriassion basin (Papadimitriou *et al.*, 2000; Papadopoulos *et al.*, 2000; Tselentis & Zahradnik, 2000; Louvari & Kiratzi, 2001), killing 143 people and causing considerable damage. Even though the magnitude of the event was M_w=6, more than 70.000 people became homeless, while thirty one buildings collapsed and hundreds were severely damaged. It may be considered as one of the most disastrous earthquakes that occurred in Greece during the last centuries. It is worth mentioning that no major ground failures were observed.

Four foreshocks, the mainshock and numerous aftershocks were recorded by the Cornet network. It should be noted that no clear evidence of seismic activity was observed in the vicinity of the Parnitha fault during the operation period of the Cornet network, until the earthquake sequence of September 1999. The foreshocks occurred within a time span of 18 min (the first 18 min and the last 2 min) before the mainshock (Fig. 10). The locations of the mainshock (Table 3), as well as of the foreshocks reported by different seismological institutes, vary significantly. Thus, the relocation of the foreshocks and of the mainshock was necessary for the interpretation of the rupture process. A well located aftershock was selected and used as a master event to relocate the mainshock and the four foreshocks. The master event was used to estimate systematic delays for the first arrivals of the Cornet stations. Arrival times from two stations of GI-NOA (ATH and PTL) were also used. The final obtained hypocenter locations were very stable, clustered within less than 1 km around 38.105°N, 23.565°E. The relocated epicenter of the mainshock is very close to the initial location obtained using data only by the Cornet network. The USGS location lies in the same area, slightly to the north. On the other hand, the obtained epicenter is significantly different from the ones proposed by NOA, PDE and HRV that are shifted about 10 km to the east. The same procedure was followed for the four foreshocks that were relocated very close to the mainshock (Fig. 10). This result significantly differs from the foreshock locations in available catalogues, where they are dispersed in the broader epicentral area. The obtained solutions suggest that the hypocenters of the mainshock and of the foreshocks are located at the deep western edge of the fault plane.

The seismic moment M_0 and the moment magnitude M_W of the Athens 1999 earthquake were obtained via spectral analysis using recordings of the stations of the Cornet network. In Fig. 11 the spectra of the E-W component of Desfina and Sofiko stations are presented. After the determination of the spectral amplitude Ω_0, the value of the seismic moment was found equal to $M_0=1\bullet10^{25}$dyn•cm, resulting a moment magnitude M_W=6.0. Furthermore, the corner frequency was f_0=0.2 Hz, indicating that the duration of the source time function was 5 sec. In order to calculate the source parameters of the mainshock, forward modeling was used. The obtained solution for the focal mechanism is strike=105°, dip=55° and rake=−80°. The focal depth was estimated 9 km and the seismic moment $M_0=1\bullet10^{25}$dyn·cm, resulting to M_W=6.0. This value of seismic moment is the same with the one obtained using spectral analysis of the Cornet recordings. An important result of the analysis was the source directivity effect towards the east (Papadimitriou et al., 2002).

The contribution of the Cornet seismological network to the study of the Athens aftershock sequence was significantly important. The joint catalogue that was formed included 50% more events than the respective of GI-NOA (Fig. 12). Specifically, the GI-NOA catalogue contained 241 events (Fig.12a), while the respective one that has been unified and homogenized through a single event algorithm included 407 events of M≥2.0 for a time interval of three months (Fig.12b). A primary concentration of the epicentres has been achieved in

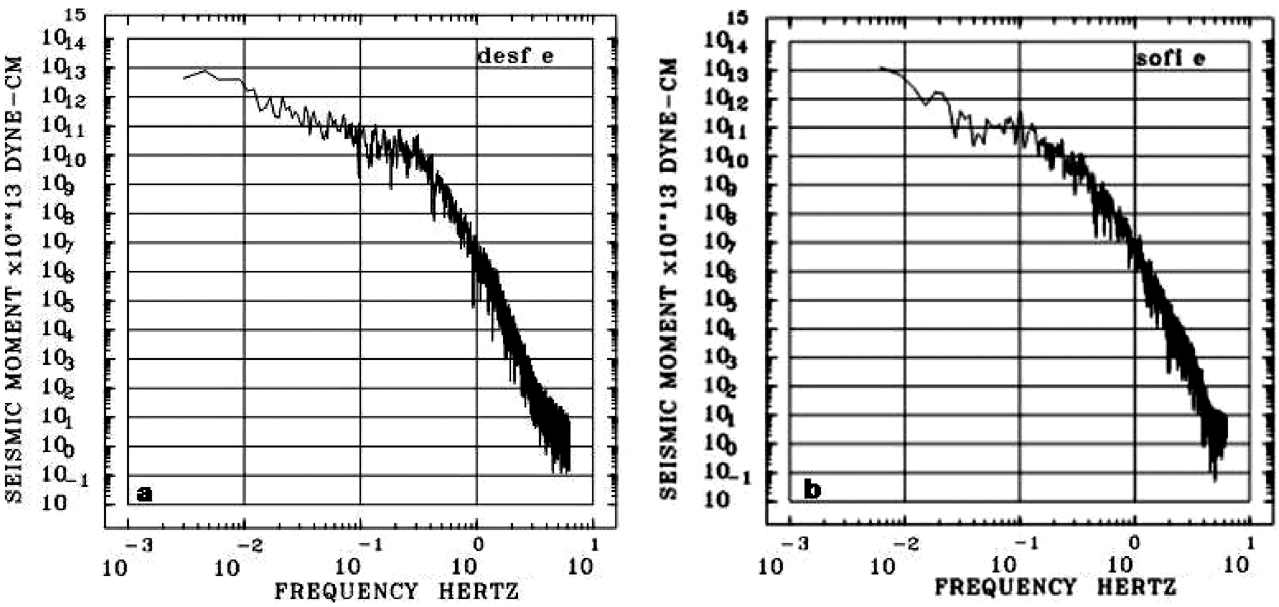

Fig. 11. Spectral analysis for the calculation of the moment magnitude of the Athens earthquake (7 September 1999) using recordings of a) Desfina and b) Sofiko stations.

the broader area of Parnitha, where the surface fault zones of Thriassion and Phyli are located.

The epicenter of the Athens Earthquake obtained by the double-difference algorithm procedure was located in Thriassion basin at a depth of 9.4 km, close to the one calculated using forward modeling. Out of the 407 earthquakes of the sequence (Fig. 13a), with mean rms and spatial errors (erx, ery, erz) equal to 0.81 sec, 3.4, 4.1 and 12.1 km, 353 were relocated (Fig. 13b) with the respective errors reduced to 0.12 sec and 1.9, 2.1 and 2.6 km (erx, ery, erz). As it can be seen in Fig. 13c, using HYPOINVERSE a better concentration of events is achieved around the main rupture zone than with HYPO71. Following this process, the mean temporal residual (rms) reached 0.36 sec, while the respective spatial ones were determined as 4.6, 5.1 and 18.2 km (erx, ery, erz). After the relocation (Fig. 13d), the mean temporal (rms) and spatial errors (erx, ery, erz) were significantly reduced. The mean rms value was equal to 0.06 sec and mean erx, ery, erz reached 1.1, 1.2 and 1.6 km, respectively. The optimization of the final results leads to clustering of the earthquake sequence in two main areas. The first one is located WNW of the mainshock epicenter, while the second one east of it (Karakonstantis & Papadimitriou, 2010).

The epicenters in Figs 13a, c are located within an extended area, whereas the relocated ones (Fig. 13b, d) are mainly concentrated close to the activated Parnitha fault escarpment (Karakonstantis, 2009). In addition, a smaller cluster located NE of the epicentral area could be related to the Phyli's fault. The obtained results were successfully compared with the ones by Papadimitriou *et al.* (2002). A local network had been deployed to record the aftershock sequence and more than 3.500 events were manually located (Pyrli, 2001). The existence of two main clusters is shown in the rose diagrams of azimuth and dip orientation distribution by

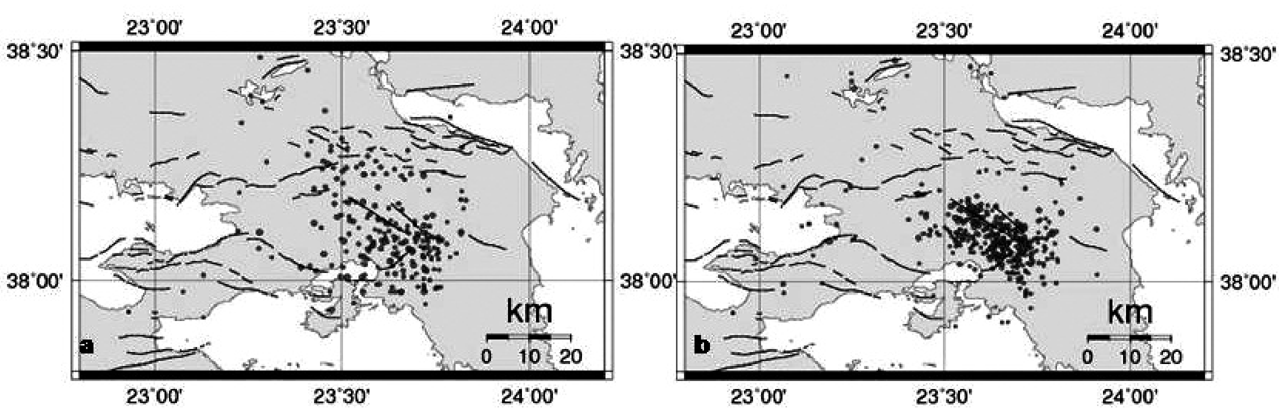

Fig. 12. Epicenters of the Athens aftershock sequence a) GI-NOA, b) Joint catalogue.

VOULGARIS *et al*. (2001) and in the focal mechanisms that were determined by PAPADIMITRIOU *et al*. (2002) in the area. An anisotropy study was also performed using data of this local network (PAPADIMITRIOU *et al.*, 2000). Mean anisotropy directions at all stations were found almost parallel to the azimuth of the main fault. The observed anisotropy is in agreement with the stress field of Western Attica and can be explained by the extensive dilatancy anisotropy (EDA) model.

A tomography study was performed in Attica region, using LOTOS code (KOULAKOV, 2009), by inverting first arrival times, including the aftershock sequence of the Athens earthquake. From the original dataset of the joint catalogue (823 events), earthquakes including at least 6 phases and ratio of S to P residual <1.5 sec were selected. The final dataset that was used for the inversion consisted of 690 earthquakes. Inversion was performed both for V_P-V_S and V_P-V_P/V_S, in order to obtain additional constraints for the amplitudes of P- and S-wave velocity anomalies. The source locations and the 1D velocity model, determined by the available software, were used as starting parameters for the nonlinear tomographic inversion. This procedure was performed in several iterations and the final result included a 3-D model (V_P, V_S and V_P/V_S ratio) comprising of horizontal slices. Taking them into account, a cross-section is performed perpendicular to the main fault (Fig. 14). Thickening of the absolute values of V_P/V_S ratio isolines is observed, at about 19 km to the SSW (arrow). The V_P/V_S ratio values vary between 1.85 to the NNE and 1.65 to the SSW, in an area of less than 3 km length, included in the parallelogram of Fig. 14. This discontinuity separates two major anomalies, one with low V_P/V_S values, close to 1.7, and the other with high values, close to 2. These anomalies can be interpreted as lateral changes in rock type and fracturing that control fluid diffusion and variation in pore pressure. Therefore, the activation of a main fault dipping south is evident, in accordance with the results obtained by PAPADIMITRIOU *et al*. (2002).

TEMPORARY NETWORKS AROUND THE GULF OF CORINTH

The Seismological Laboratory of the University of Athens has participated in numerous national and international research projects, mainly in Central Greece. Several temporary seismological networks were installed in the broader area of the Gulf of Corinth since 1990, to record either background seismicity (RIGO *et al*., 1996; PAPADIMITRIOU *et al*., 2001), or aftershock sequences of large events, as the 1992 Galaxidi (KEMEZENTZIDOU *et al*., 1993) and the 1995 Aigion (BERNARD *et al*., 1997) earthquakes.

Specifically, in July-August 1991, a seismological network was installed around the western Gulf of Corinth with

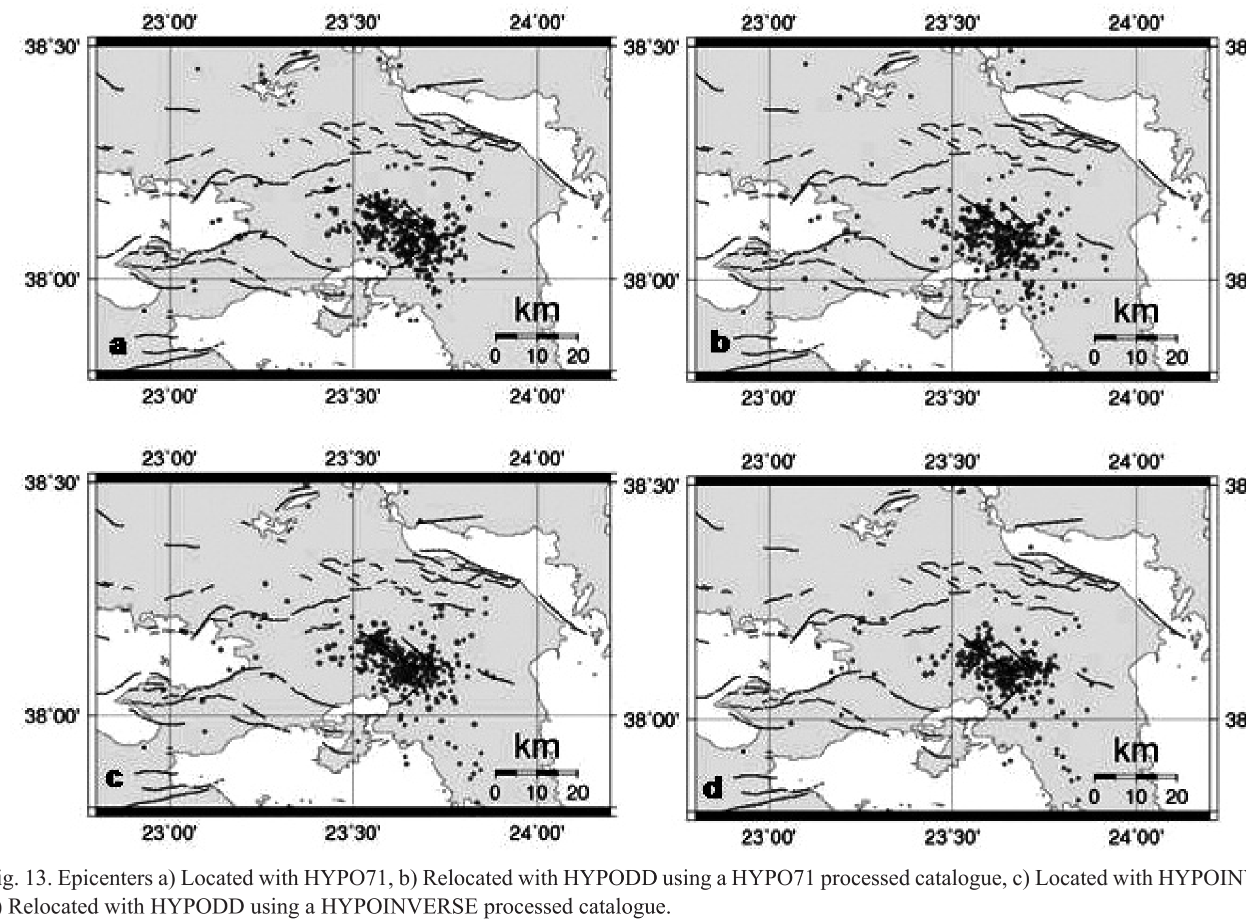

Fig. 13. Epicenters a) Located with HYPO71, b) Relocated with HYPODD using a HYPO71 processed catalogue, c) Located with HYPOINVERSE, d) Relocated with HYPODD using a HYPOINVERSE processed catalogue.

the collaboration of the Universities of Athens, Paris and Grenoble, in order to monitor the microseismic activity of the area. This network consisted of 60 digital stations of different types (RIGO *et al*., 1996). The determination of focal mechanisms and the crustal structure of the area through ray-tracing (PAPADIMITRIOU *et al*., 1994a) contributed to the seismotectonic analysis of the broader area of the western part of the Gulf of Corinth. In November 1992, a network of 35 portable seismographs was installed in the area of Galaxidi for a period of 10 days (PAPADIMITRIOU *et al*., 1994b; HATZFELD *et al*., 1996) in order to study the aftershock sequence of the mainshock (Ms=5.9, 18/11/1992). After the occurrence of the Aigion earthquake (Ms=6.2, 15/6/1995) a network that consisted of 24 GPS points and 20 digital seismographs was installed to constrain the rupture geometry (BERNARD *et al*., 1997). During the summer of 1992, a temporary network of 68 seismological stations operated in Central Greece, in the regions of Thessaly and Evia. The network recorded 510 earthquakes and 80 focal mechanisms were determined (HATZFELD *et al*., 1999a). In the following year (1993), a seismological network was installed (HATZFELD *et al*., 1999b) for a period of 7 weeks around the eastern Gulf of Corinth, where a sequence of strong earthquakes occurred in 1981. This network consisted of 36 smoked-paper Sprengnether MEQ 800 stations and 18 Reftek digital data loggers. The determined focal mechanisms revealed normal faulting.

Since 2000, an in situ laboratory for obtaining data on the physics of earthquakes and fault mechanics was established in Aigion area, in the western Gulf of Corinth (DOAN & CORNET, 2007; CORNET *et al*., 1998). A 1000m deep borehole was drilled to study the Aigio fault. The well intersects it between 760 and 770 m. The dip of the fault is 60° and does not seem to change with depth. Coring and various logs have been performed to constrain the geological and geophysical environment of the fault. Pore pressure in the well has been continuously measured from September 2003 to early 2005. The Corinth Rift Laboratory (CRL) that was developed in

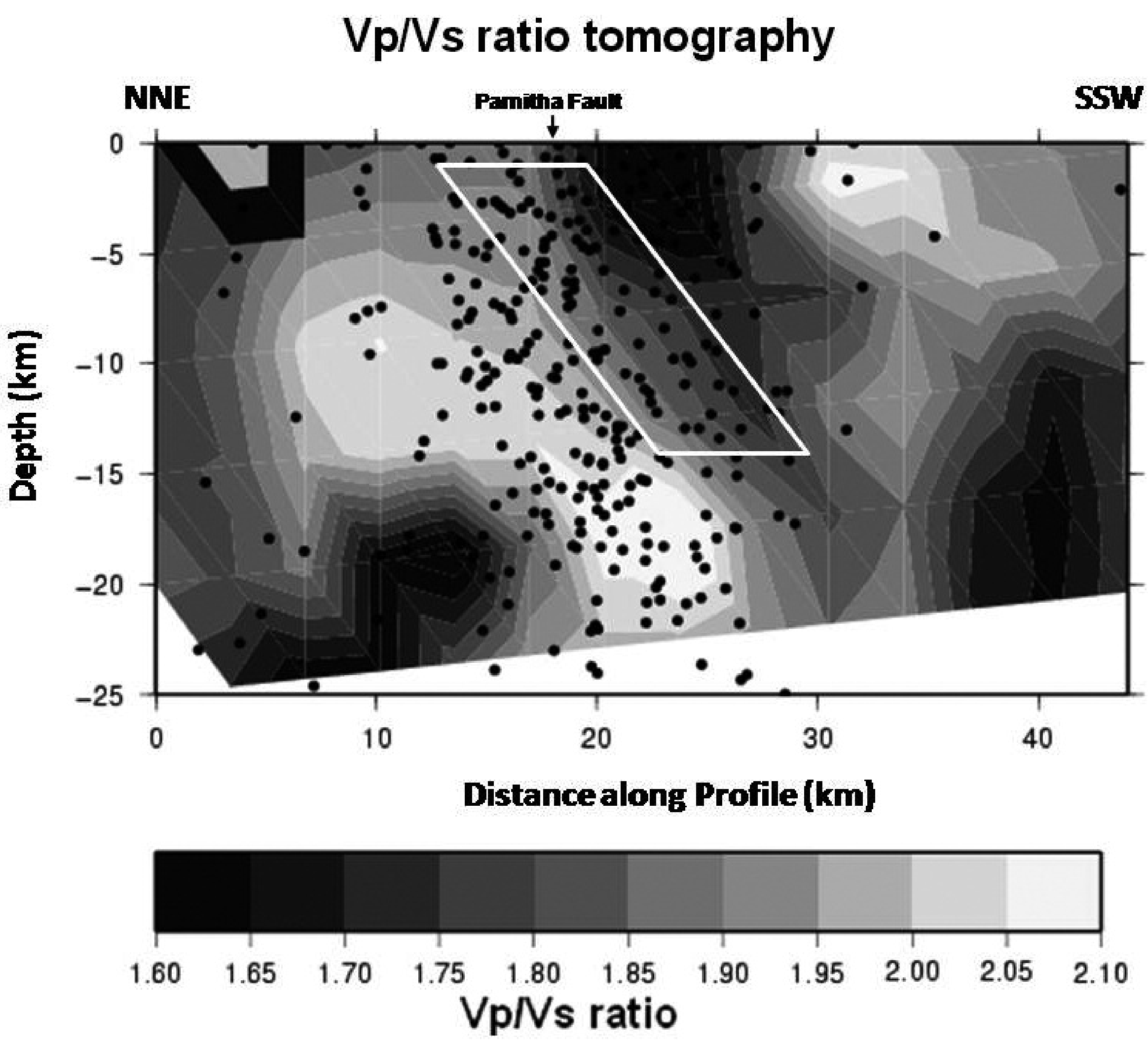

Fig. 14. Tomographic cross-section NNE-SSW Vp/Vs ratio, where hypocenters are presented (circles). The parallelogram includes an area of high Vp/Vs contrast, indicating the presence of the activated Parnitha fault, whose projection on surface is also indicated (arrow).

the area of the western Gulf of Corinth, involves continuous monitoring of strain, seismicity, fluid pressure and geochemistry. It was carried out both at surface and at various depths in boreholes intersecting active faults. Well imaging has been repeatedly carried out to study the fractures and their relationship with stress variations. This laboratory is centered on the south shore of the Corinth rift near the city of Aigion. The studied faults affect Cretaceous carbonate rocks, which constitute a classical fractured hydrocarbon reservoir (Bernard *et al*., 2006).

THE CORINTH 1996 NETWORK

Results concerning both seismicity and focal mechanisms that were obtained from all the above mentioned temporary networks have already been published. Another important research project was performed via the Corinth 1996 network, from which only analysis of teleseismic events has been published (Tiberi *et al*., 2000). For that reason the results obtained for the local events are included in the present study.

The Corinth 1996 temporary seismological network was installed, with the collaboration of French and Greek institutes, in June 1996 and operated for six months, until December 1996, along 2 profiles starting from Peloponnesus to North Evia. The network consisted of 60 stations installed at 44 sites (Fig. 15), with a mean spacing of about 10 km, organized into two main sub parallel profiles. The stations of the western profile were operating in continuous mode, equipped with 3D Titan stations, while the eastern ones in triggering mode, comprising of Hades 3D and Minititan 1D seismographs. The goal of the installation of this network was the study of the local seismic activity and the tectonic regime. Furthermore, 177 teleseismic events were recorded and gave more than 2.000 travel time (P and PKP phases) residuals, which were inverted to image the velocity structure (Tiberi *et al*., 2000).

Data recorded by the Corinth 1996 network were combined with those recorded by the Cornet network. In Fig. 16 the epicentres of the 649 located events, using HYPO71, are presented. Concentration of seismic sources was observed within the Gulf of Corinth, at Perachora, Psatha, Villia, Atalanti, Yliki lake and Evia. At least two clusters can be distinguished at the northern part of the Gulf of Corinth that can be related to the seismogenic zones of Galaxidi and Aigion, respectively, and one cluster at the southern part, north of the cities of Xylokastro and Kiato.

Following, using the first P-wave polarities method and recordings of both the Corinth 1996 and the Cornet networks, 170 focal mechanisms were constrained, 34 of which were synthetic. The 95 best determined fault plane solutions are presented in Fig. 17. The ones located in the Gulf of Corinth revealed normal faulting trending almost E-W. These solutions are in agreement with the direction of the main active faults of the area, as well as with the geomorphology of the Gulf. In the broader Atalanti area, focal mechanisms present a general WNW-ESE direction, consistent with the main direction of the Atalanti fault which dominates the region.

THE ATHENET NETWORK

The Cornet network operated until 2004, when the first stations of the Athenet broadband network of the Seismological Laboratory of the University of Athens were installed in the broader area of Central Greece. Currently, the Athenet network consists of 22 permanent stations. In 2008 the Hellenic Unified Seismological Network (HUSN) started operating, comprising of the networks of the Universities of Athens, Thessaloniki and Patras, as well as of the Geodynamic Institute of the National Observatory of Athens. The operation of HUSN was of great importance, since even events with M<2.0 are detected in the majority of continental Greece. Furthermore, a database of continuous broadband recordings has been created and can be used for research purposes. It is worth noticing that until now more than 50.000 earthquakes have been located. Automatic procedures have been developed for both hypocenter and magnitude determination,

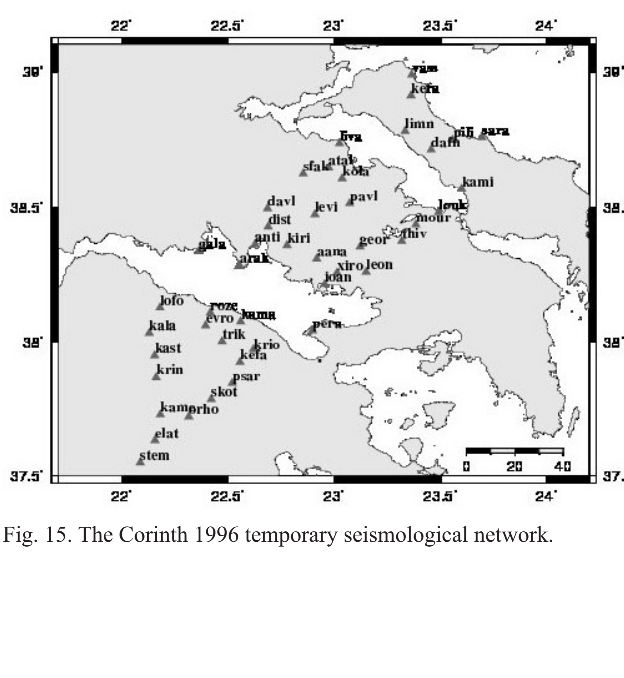

Fig. 15. The Corinth 1996 temporary seismological network.

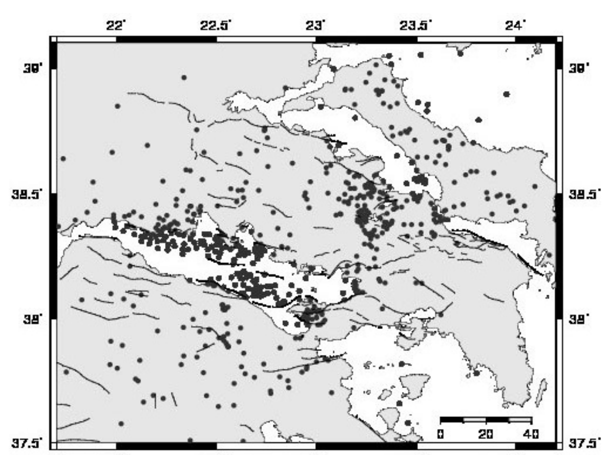

Fig. 16. Seismicity located using recordings of the Corinth 1996 and the Cornet networks.

which are provided in real time. In addition, source parameters for moderate events are determined applying moment tensor inversion using regional waveforms (Moshou *et al.*, 2010). The results of the above mentioned analysis are published in http://www.geophysics.geol.uoa.gr.

CONCLUSIONS

The seismic activity in the Gulf of Corinth is significantly high and has caused severe damages since the antiquity, while during the last two decades the population of the coastal areas of the Gulf has grown, resulting to the increase of the seismic risk of the region. The absence of permanent seismological stations led the Seismological Laboratory of the University of Athens to focus in this area by installing the first digital seismological network, Cornet, around the eastern Gulf of Corinth. Recently, the Athenet broadband network was developed and covers the entire Gulf of Corinth, as well as Central Greece.

For the best possible determination of the source parameters, a velocity model that consists of six (6) seismic layers was obtained. The microseismic activity was recorded in a very detailed way. Concentration of seismic sources was observed within the Gulf of Corinth forming several clusters, while important seismicity occurred close to the Cornet stations. During the operation period of the Cornet network

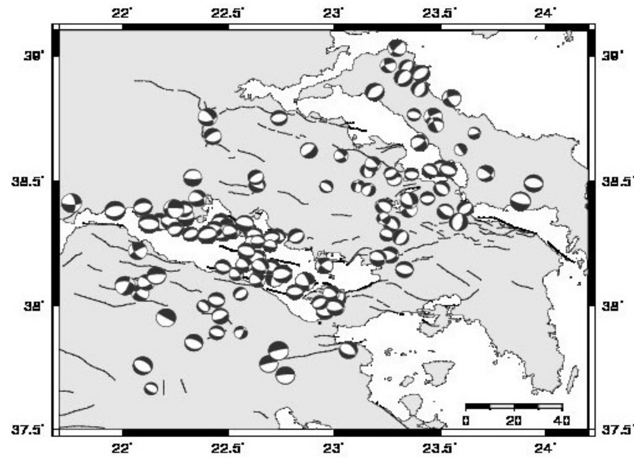

Fig. 17. Selected focal mechanisms using recordings of the Corinth 1996 and the Cornet networks.

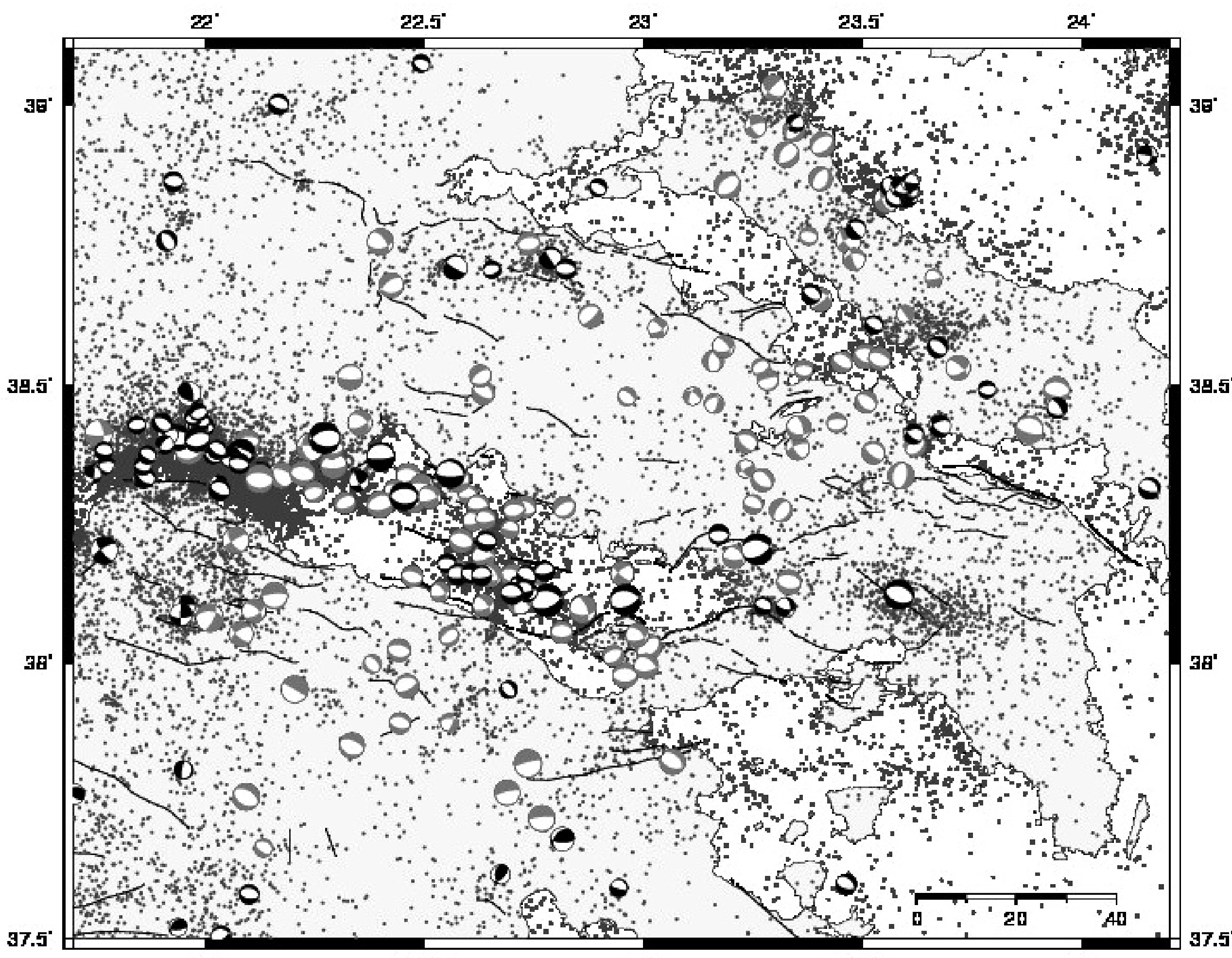

Fig. 18. Seismotectonic map of Central Greece.

more than 6.000 events have been located, the majority of which is situated in the Gulf of Corinth. Following, the Cornet data were unified and homogenized with GI-NOA and AUTH phases, resulting to a more complete earthquake catalogue. A relocation procedure has been applied for specific areas leading to the minimization of location errors. For a rapid magnitude estimation, linear multiple regression was applied to determine the constants for the calculation of the duration magnitude M_D. Following, the moment magnitude M_W, which is considered to be the most reliable magnitude scale, was calculated using spectral analysis, a catalogue was created and a relation between these two magnitude scales was determined. Fault plane solutions that were constrained in the Gulf of Corinth indicate normal faulting mainly striking in an E-W direction.

Analysis of data recorded by the Cornet network revealed the existence of an anisotropic upper crust around both parts of the Gulf of Corinth. The uniformity of the fast shear wave polarizations that were determined at all stations, irrespective of the azimuth of each event, is consistent with what is expected for shear-wave splitting due to propagation through an anisotropic medium. These observations are consistent with the general NNE-SSW direction of extension of the Gulf and, therefore, in agreement with the extensive dilatancy anisotropy (EDA) model.

The Athens 1999 earthquake, as well as its foreshocks, were relocated using a master event and were found in the same focal area. It is worth noticing that the relocated epicenter of the mainshock was very close to the initial location obtained using only Cornet data. A relocation procedure was applied for the aftershocks of the Athens earthquake, using the HYPODD algorithm. Two separated clusters were distinguished, the first west and the second east of the mainshock location. Local earthquake tomography was performed in Attica, with phase data from the joint catalogue. This procedure revealed the activation of a main fault dipping south, in agreement with the relocated hypocentral distribution.

The permanent seismological networks operated by the Seismological Laboratory of the University of Athens contribute to accurately locate the microearthquakes, to determine their source parameters and to reveal the main seismotectonic characteristics of the active structures. The seismotectonic map of Central Greece, presented in Fig. 18, was created using the previously mentioned joint catalogue. The main active faults of the region and focal mechanisms, determined both using a moment tensor inversion technique (black colour) and first P-wave polarities (grey colour), are also presented. Fault plane solutions, associated with the observed clustering of seismicity, can be related to the active surface faults.

REFERENCES

ARMIJO, R., MEYER, B., KING, G.C.P., RIGO, A. & D. PAPANASTASSIOU (1996). Quaternary evolution of the Corinth Rift and its implications for the late Cenozoic evolution of the Aegean. *Geophys. J. Int*., 126, 11-53.

BERNARD, P., BRIOLE, P., MEYER, B., LYON-CAEN, H., GOMEZ, J.-M., TIBERI, C., BERGE, C., CATTIN, R., HATZFELD, D., LACHET, C., LEBRUN, B., DESCHAMPS, A., COURBOULEX, F., LARROQUE, C., RIGO, A., MASSONET, D., PAPADIMITRIOU P., KASSARAS, J., DIAGOURTAS, D., MAKROPOULOS, K., VEIS, G., PAPAZISI, E., MITSAKAKI, C., KARAKOSTAS, V., PAPADIMITRIOU, E., PAPANASTASSIOU, D., CHOULIARAS, M. & G. STAVRAKAKIS (1997). The M_S=6.2, June 15, 1995 Aigion Earthquake (Greece): evidence for a low angle normal faulting in the Corinth Rift. *Journ. Seismology*, 1, 131-150.

BERNARD, P., LYON-CAEN, H., BRIOLE, P., DESCHAMPS, A., PITILAKIS, K., MANAKOU, M., BOUDIN, F., BERGE, C., MAKROPOULOS, K., DIAGOURTAS, D., PAPADIMITRIOU, P., LEMEILLE, F., PATAU, G., BILLIRIS, H., CASTAREDE, H., CHARADE, O., NERCESSIAN, A., AVALLONE, A., ZAHRADNIK, J., SACKS, S. & A. LINDE (2006). Seismicity, deformation and seismic hazard in the western rift of Corinth: New insights from the Corinth Rift Laboratory (CRL). *Tectonophysics*, 426 (1-2), 7-30.

BILLIRIS, H., PARADISSIS, D., VEIS, G., ENGLAND, P., FEATHERSTONE, W., PARSONS, B., CROSS, P., RANDS, P., RAYSON, M., SELLERS, P., ASHKENAZI, V., DAVISON, M., JACKSON, J. & N. AMBRASEYS (1991). Geodetic determination of tectonic deformation in central Greece from 1900 to 1988. *Nature*, 350, 124-129.

BOOTH, D. C. & S., CRAMPIN (1985). Shear wave polarizations on a curved wavefront at an isotropic free surface. *Geophys. J. R. Astron*. Soc., 83, 31-45.

BOUIN, M.P., TELLEZ, J. & P. BERNARD (1996). Seismic anisotropy around the Gulf of Corinth, Greece, deduced from three-component seismograms of local earthquakes and its relationship with crustal strain. *J. Geophys. Res.*, 101, 5797-5811.

BROOKS, M. & G. FERENTINOS (1984). Tectonics and sedimentation in the Gulf of Corinth and the Zanthe and Cephalonia channels, western Greece. *Tectonophysics*, 101, 25-54.

BRIOLE, P., RIGO, A., LYON-CAEN, H., RUEGG, J.-C., PAPAZISSI, K., MITSAKAKI, C., BALODIMOU, A., VEIS, G., HATZFELD, D. & A. DESCHAMPS (2000). Active Deformation of the Corinth Rift, Greece: Results from Repeated GPS Surveys between 1990 and 1995. *J. Geophys. Res*., 105, 256-5-256-156.

CORNET, F.H., BORM, G., MCEVILLY, T. & I.VARDOULAKIS (1998). Proceedings of the 1st workshop on the development of a multiborehole observatory at the Gulf of Corinth; *ICDP Report 1996/1997*, GFZ-Potsdam publ., 28-103 p.

CRAMPIN, S. (1978). Seismic-waves propagation through a cracked solid: polarization as a possible dilatancy diagnostic. *Geophys J. R. Astr. Soc.*, 53, 467-496.

CRAMPIN, S. (2003). The New Geophysics: shear-wave splitting provides a window into the crack-critical rock mass. *The Leading Edge*, 22, 536-549.

CRAMPIN, S., VOLTI, T. & R., STEFANSSON (1999). A succesfully stress-forecast earthquake. *Geophys. J. Int.*, 138, F1-F5.

CROSSON, R., (1976). Crustal structure modeling of earthquake data. 1. Simultaneous least squares estimation of hypocenter and velocity parameters. *J. Geophys. Res*., 81, 3036-3046.

DOAN, M.L., & F.H., CORNET (2007). Thermal anomaly near the Aigio fault, Gulf of Corinth, Greece, maybe due to convection below the fault. *Geophys. Res. Lett*., 34, L06314, 5 pp.

GAO, Y., WANG, P., ZHENG, S., WANG, M. & Y. T. CHEN (1998). Temporal changes in shear-wave splitting at an isolated swarm of small earthquakes in 1992 near Dongfang, Hainan Island, southern China. *Geophys. J. Int.*, 135, 102-112.

HANKS, T. C., & H., KANAMORI (1979). A moment magnitude scale. *J. Geophys. Res.*, 84, 2348-2350.

HAO, P., GAO, Y. & S., CRAMPIN (2008). An Expert System for measuring shear-wave splitting above small earthquakes. *Comp. Geosci*., 34, 226-234.

HATZFELD, D., KEMENTZETZIDOU, D., KARAKOSTAS, V., ZIAZIA, M., NOTHARD, S., DIAGOURTAS, D., DESCHAMPS, A., KARAKAISIS, G., PAPADIMITRIOU, P., SCORDILIS, M., SMITH, R., VOULGARIS, N., KIRATZI, S., MAKROPOULOS, K., BOUIN, M. P., & P. BERNARD (1996). The Galaxidi Earthquake of 18 November 1992: A Possible Asperity within the Normal Fault System of the Gulf of Corinth (Greece). *Bull. Seism. Soc. Am.*, vol. 86, 6, 1987-1991.

HATZFELD, ZIAZIA, M., KEMEZENTZIDOU, D., HATZIDIMITRIOU, P., PANAGIOTOPOULOS, D., MAKROPOULOS, K., PAPADIMITRIOU, P. & A., DESCHAMPS (1999a). Microseismicity and focal mechanisms at the western termination of the North Anatolian Fault and their implications for continental tectonics. *Geophys. J. Int*., 137, 891–908.

HATZFELD, D., KARAKOSTAS, V., ZIAZIA, M., KASSARAS, I., PAPADIMITRIOU, E., MAKROPOULOS, K., VOULGARIS, N. & C. PAPAIOANNOU (1999b). Microseismicity and faulting geometry in the Gulf of Corinth (Greece), *Geophys. J. Int*., 141, 438–456.

JACKSON, J. A., GAGNEPAIN, J., HOUSEMAN, G., KING, G. C. P., PAPADIMITRIOU, P., SOUFLERIS, C. & J. VIRIEUX, (1982). Seismicity, normal faulting and the geomorphological development of the Gulf of Corinth (Greece): the Corinth earthquakes of February and March 1981. *Earth planet. Sci. Lett.,* 57, 377-397.

KANASEWICH, E. R. (1981). *Time sequence analysis in Geophysics*. Univ. of Alberta Press, Edmonton, Alberta.

KANESHIMA, S. (1990). Origin of crustal anisotropy: Shear wave splitting studies in Japan. *J. Geophys. Res*., 95, 11121-11133.

KARAKONSTANTIS, A. (2009). Unification-Homogenization of seismological catalogues and re-assessment of focal parameters of earthquakes during 1996-2006 period. Application to Seismotectonics of the Hellenic peninsula, *Master thesis*, Geophysics-Geothermics Department, Faculty of Geology, University of Athens, Greece, 262 pp. (in Greek).

KARAKONSTANTIS, A., & P. PAPADIMITRIOU (2010). Earthquake relocation in Greece using a unified and homogenized seismological catalogue. *Bull. Geol. Soc. Greece,* Proc. of the 12th International Congress, Patras, May 2010, XLIII, No 4, 2043-2052.

KAVIRIS, G. (2003). Study of Seismic Source Properties of the Eastern Gulf of Corinth. *Ph. D. Thesis*, Geophysics-Geothermics Department, Faculty of Geology, University of Athens, Greece (in Greek).

KAVIRIS, G., PAPADIMITRIOU, P. & K. MAKROPOULOS (2007). Magnitude Scales in Central Greece. *Bull. Geol. Soc. Greece*, XXXX, part 3, 1114-1124.

KAVIRIS, G., PAPADIMITRIOU, P. & K. MAKROPOULOS (2008). An Overview of Anisotropy Studies in Central Greece using recordings around the Gulf of Corinth (Greece) and aftershocks of the 1999 Athens Earthquake. *31st General Assembly of the ESC 2008*, Short Papers, pg 215-223.

KEMEZENTZIDOU, D., BERNARD, P., BOUIN, M.-P., DERVIN, P., DIAGOURTAS, D., HATZFELD, D., KARAKAISIS, G., KARAKOSTAS, B., NORTHARD, S., PAPADIMITRIOU, E., SCORDILIS, E., SMITH, R., VOULGARIS, N. & M. ZIAZIA (1993). Aftershock study of the Galaxidi earthquake of November 18, 1992. *Bull. Seism. Soc. Am*., 86, 1987-1991.

KIRATZI, A. (1984). Earthquake magnitude scales in the broader Aegean area. *PhD Thesis*, Univ. of Thessaloniki (in Greek).

KOULAKOV I. (2009). LOTOS code for local earthquake tomographic inversion. Benchmarks for testing tomographic algorithms, *Bull. Seis. Soc. Am.,* 99, No. 1, 194-214.

LOUVARI, E. & A. KIRATZI (2001). Source parameters of the 7 September 1999 Athens (Greece) earthquake based on teleseismic data. J. *Balk. Geoph. Soc.*, 4, n. 3, 51-60.

MELIS, N.S., BROOKS, M. & R.G. PEARCE (1989). A microearthquake study in the Gulf of Patras region, western Greece, and its seismotectonic interpretation. *Geophys. J. R. Astr. Soc*., 98, 515-524.

PAPADIMITRIOU, P., KASSARAS, I., LYON-CAEN, H., MAKROPOULOS, K. & J., DRAKOPOULOS (1994a). Seismic wave propagation and crustal structure in western Corinth gulf (C. Greece). *Proc. of the XXIV General Assembly of the ESC*, vol 1, 610-619.

PAPADIMITRIOU, P., KASSARAS, I., RIGO, A., LYON-CAEN, H., HATZFELD, D., MAKROPOULOS, K. & J., DRAKOPOULOS (1994b). Source parameters of large and small earthquakes in Corinth Gulf (C. Greece). Pr*oc. of the XXIV Gen. Ass. of ESC*, Athens, Greece, vol. II, 848-858.

PAPADIMITRIOU, P., MAKROPOULOS, K., KASSARAS, I., KAVIRIS, G. & J. DRAKOPOULOS (1996). The Eastern Corinthian Gulf (Greece) Seismological Telemetry Network (CORNET). *XXV Gen. Ass. ESC*, Reykjavik, Iceland.

PAPADIMITRIOU, P., KAVIRIS G. & K., MAKROPOULOS (1999). Evidence of shear-wave splitting in the Eastern Corinthian Gulf (Greece). *PEPI*, 114, 3-13.

PAPADIMITRIOU, P., KAVIRIS G., VOULGARIS, N. & I. KASSARAS, (2000). Shear-wave splitting analysis using aftershocks of the 7th September 1999 Earthquake: Preliminary Results. *Ann. Geol. Pays Hellen*., XXXVII, FASC. B, 89-103.

PAPADIMITRIOU, P., KAVIRIS, G., CHOUNTIS, P., CHOUSIANITIS, K., MILESIS D., XENIKAKIS, TH., MAKROPOULOS, K., TIBERI, C. & H. LYON-CAEN (2001). Seismicity and fault mechanics in the region of Corinth and Evvia Rift System (Greece). *EGS XXVI General Assembly, Nice, France*, Book of Abstracts, 1546.

PAPADIMITRIOU, P., KAVIRIS G., VOULGARIS, N. & I. KASSARAS (2000). Shear-wave splitting analysis using aftershocks of the 7th September 1999 Earthquake: Preliminary Results. *Ann. Geol. Pays Hellen*., T. XXXVII, FASC. B, 89-103.

PAPADIMITRIOU, P., VOULGARIS, N., KASSARAS, I., KAVIRIS, G., DELIBASIS, N. & K. MAKROPOULOS (2002). The M_W=6.0, 7 September 1999 Athens Earthquake. *Natural Hazards*, 27, 15-33.

PAPADOPOULOS, G., DRAKATOS, G., PAPANASTASSIOU, D., KALOGERAS, I. & G. STAVRAKAKIS (20000. Preliminary results about the catastrophic earthquake of 7 September 1999 in Athens, Greece. *Seismol. Res. Lett*., 71, 318–329.

PAPANASTASSIOU, D. (1989). Detectibility and accuracy of source parameters determination of the networks of N.O.A. *PhD Thesis*, Univ. of Athens (in Greek).

PAPAZACHOS, B. & K. PAPAZACHOU (1989). *Earthquakes in Greece*. Ziti Editions, Thessaloniki, 356 pp.

PAPAZACHOS, B. C., KIRATZI, A. A., & B. G., KARAKOSTAS (1997). Toward a Homogeneous Moment-Magnitude Determination for Earthquakes in Greece and the Surrounding Area. *Bull. Seism. Soc. Am.*, 87, No. 2, 474-483.

PYRLI, M. (2001). Seismotectonic characteristics of the aftershock sequence of the Athens earthquake. *M.Sc.*, Geophysics-Geothermics Department, Faculty of Geology, University of Athens, Greece (in Greek).

RIGO, A., LYON-CAEN, H., ARMIJO, R., DECHAMPS, A., HATZFELD, D., MAKROPOULOS, K. AND P. PAPADIMITRIOU (1996). A microseismic study in the western part of the Gulf of Corinth (Greece): implications for large scale normal faulting mechanisms. *Geophys. J. Int*., 126, 663-688.

TIBERI, C., LYON-CAEN, H., HATZFELD, D., ACHAUER, U., KARAGIANNI, E., KIRATZI, A., LOUVARI, E., PANAGIOTOPOULOS, D., KASSARAS, I., KAVIRIS, G., MAKROPOULOS K. AND P. PAPADIMITRIOU (2000). Crustal and upper mantle structure beneath the Corinth rift (Greece) from a teleseismic to-

mography study. *J. Geophys. Res*., 105, No B12, 28159-28171.
TSELENTIS, G.-A. (1997). Contemporary Seismology. *Publ. Papasotiriou*, Athens (in Greek).
TSELENTIS, G.-A. & J. ZAHRADNIK (2000). The Athens Earthquake of 7 September 1999. *Bull. Seism. Soc. Am*., 90, n. 5, 1143-1160.
VOULGARIS, N., PIRLI, M., PAPADIMITRIOU, P., KASSARAS, I. & K. MAKROPOULOS (2001). Seismotectonic Characteristics of the Area of Western Attica derived from the study of the September 7, 1999 Athens Earthquake Aftershock Sequence. *Bull. Geol. Soc. of Greece*, XXXIV, no 4, 1645-1654.